

PHASE DISPLACEMENT IN PNEUMATIC TRANSPORT WITH A DENSE MEDIUM

M. B. Rivkin and V. A. Sorochinskii

UDC 621.867.8

The results are shown of an experimental study concerning pneumatic transport with a dense medium by various routes. It is shown that adding complexity to the route results in a phase displacement at the entrance to the duct.

The characteristics of pneumatic transport with a dense medium of high admixture concentration are very different than those of ordinary pressurized pneumatic transport with a low admixture concentration [1, 2, 3].

A special feature of the pneumatic transport process with a dense medium is the self-regulating accessory equipment (e.g., the compressor pumps), i.e., that for each transport route at a specific flow rate the transport mode is established – automatically – to perform in accordance with any specific conditions.

Changing the route, or increasing or decreasing the air flow rate, results in a corresponding change of discharge pressure and discharge efficacy.

This fact, although mentioned by several authors [4, 5], has not yet been explained satisfactorily.

The unavailability of sufficient experimental data which would reveal the physical character of the processes taking place here makes it impossible to develop a generally acceptable method of designing pneumatic transport equipment for such a dense medium, which is an obstacle in making this pneumatic transport technique more widespread.

In order to detect the basic relations underlying the operation of pneumatic transport with a dense medium, a laboratory model of a compressor pump was built for periodic duty with discharge on top (Fig. 1). The apparatus consisted of an air chamber 1, a transport duct 2, and a receiving tank 3. The air chamber was cylindrical, $D = 300$ mm in diameter and $h = 1500$ mm high. In the lower part of the air chamber there was installed a porous partition 4. The transport duct 2 was made of steel with an inside diameter $D_T = 20$ mm and with several glass segments for visual inspection and cinematographic recording of the air-dust mixture flow. The entrance segment of the duct was conically divergent and separated from the porous partition by a $h_0 = 60$ mm clearance.

Inside the upper part of the receiving tank 3 there was installed a cloth filter 9 to ensure a fine purification of the exhaust air. The receiving tank and the air chamber were connected through a flexible overflow tube, along which and through a valve 6 the charge was returned to the air chamber 1.

As the charge material we used apatite concentrate – a multidispersed dust with the average particle size $d_p = 60 \mu\text{m}$. The moisture content in the apatite concentrate was 0.3–0.4% by weight. The following process parameters were recorded oscillographically during the pneumatic transport tests:

- a) the mass flow rate of air (G_a);
- b) the air pressure ahead of the measuring diaphragm (P_0), underneath the porous partition (P_1), in the upper zone of the air chamber above the charge (P_2), and in the receiving tank (P_3);
- c) the discharge efficacy (G_m);
- d) the density of the air-dust mixture (ρ) at the entrance section to the transport duct;

Translated from *Inzhenerno-Fizicheskii Zhurnal*, Vol. 20, No. 6, pp. 1072–1077, June, 1971. Original article submitted April 7, 1970.

© 1973 Consultants Bureau, a division of Plenum Publishing Corporation, 227 West 17th Street, New York, N. Y. 10011. All rights reserved. This article cannot be reproduced for any purpose whatsoever without permission of the publisher. A copy of this article is available from the publisher for \$15.00.

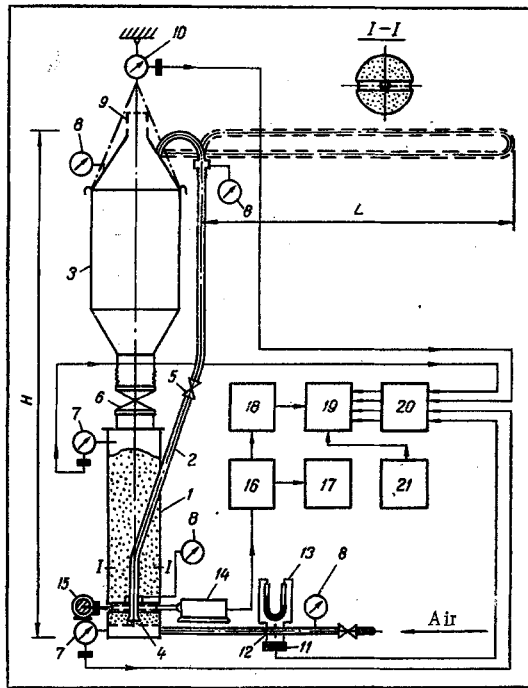


Fig. 1. Schematic diagram of the test apparatus: 1) air chamber, 2) transport duct, 3) tank, 4) porous partition, 5, 6) sampling valves, 7) pressure gage, 8) manometer, 9) filter, 10) weight gage, 11) pressure-drop gage, 12) diaphragm, 13) U-tube manometer, 14) γ -radiation receiver, 15) γ -radiation source, 16) amplifier, 17) model S1-4 oscilloscope, 18) demodulator, 19) model N-102 oscillograph, 20) amplifier, 21) power supply.

e) the time of unloading the air chamber (t).

For measuring the density of the air-dust mixture, a segment was set apart from the air chamber at the entrance to the transport duct and separated from the charge (Fig. 1) by a cylindrical tube containing a γ -radiation source 15 at one end and a γ -radiation pickup 14 at the other. A radioactive Cs-137 isotope 2000 mg equiv. radium strong was used as the γ -radiation source and a differential ionization chamber was used as the radiation pickup.

The signal, proportional to the air-dust mixture density, was fed to the electronic amplifier 16 and to the oscilloscope 17. The same signal, after having been passed through the demodulator 18, was recorded on the loop oscillograph 19. With the aid of a calibrating curve, the true density of the air-dust mixture was determined from the magnitude of this signal.

For plotting the calibration curve and obtaining the mass coefficient of apatite absorption, a special experimental study had been conducted in [7].

On this test apparatus we studied the pneumatic transport with a dense medium along four different routes:

- a) route No. 1 with a vertical segment $H = 2.6$ m,
- b) route No. 2 with a vertical segment $H = 2.6$ m and a horizontal segment $2L = 6.8$ m,

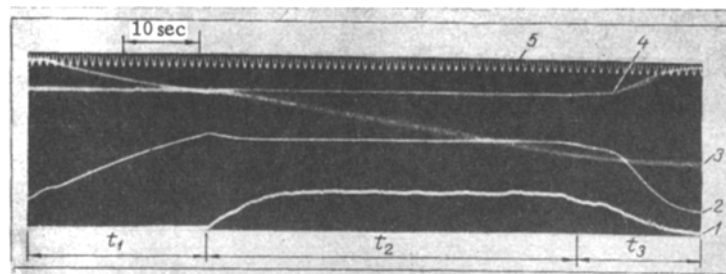


Fig. 2. Oscillogram of the transport process: 1) density of the air-dust mixture ρ (kg/m^3), 2) air pressure P_1 (N/m^2), 3) discharge efficacy G_m (Kg/h), 4) air pressure P_2 (N/m^2), 5) time t (sec).

TABLE 1. Values of the Constants A, B, C, and D for Different Transport Routes

Route No.	Values of the constants			
	A	B	C	D
1	-0,96	0,83	-2,16	2,80
2	-0,65	0,80	-3,17	5,30
3	-0,99	1,18	-4,62	7,32
4	-0,69	1,10	-5,77	12,00

c) route No. 3 with a vertical segment $H = 2.6$ m and a horizontal segment $2L = 9.2$ m,

d) route No. 4 with a vertical segment $H = 2.6$ m and a horizontal segment $2L = 18.4$ m.

For each route the test was performed under six different operating conditions (air flow rates). The discharging was done ten times for each operating mode and all tests were oscillographed.

The characteristics of the compressor pump discharge process is depicted on the oscillogram in

Fig. 2. One discharge cycle consisted of three stages: preliminary stage (air pumping) t_1 , steady-state discharge t_2 , and shut off stage t_3 .

After the oscillograms had been interpreted, the test results were evaluated and averaged. The reference air velocity w_0 , i. e. the air velocity at the entrance section referred to the duct area was used as the criterial parameter in the data evaluation. The discharge efficacy G_m and the weight concentration μ of the dust admixture are shown in Fig. 3 as functions of the air velocity w_0 for the various transport routes. It is evident from the graphs that the route configuration has a considerable effect on the pneumatic transport process parameters, and that making the route more complex (adding to the horizontal segments) will result in a lower discharge efficacy as well as a lower weight concentration of the dust admixture.

It can be seen from Fig. 3b that the air-dust mixture porosity ε_0 at the duct entrance is a single-valued function of the referred air velocity w_0 and is almost independent of the route configuration.

This relation can be represented with sufficient accuracy by the formula

$$\varepsilon_0 = \varepsilon'_0 + \beta w_0 \quad \text{for } \varepsilon'_0 = 0.7; \quad \beta = 0.007. \quad (1)$$

In Fig. 3c we show graphically how, for different transport routes, the displacement coefficient K_0 at the duct entrance varies with air velocity. This coefficient was calculated by the formula:

$$K_0 = \frac{w_a}{w_m} = \frac{\gamma_m(1 - \varepsilon_0) P_0}{\gamma_0 \varepsilon_0 P G_m} G_a. \quad (2)$$

The curve representing $K_0 = f(w_0)$ is fitted by means of the Lagrange interpolation polynomial. The sought relation can be written in the form:

$$K_0 = A(w_0)^3 + B(w_0)^2 + C(w_0) + D. \quad (3)$$

The values of the constants A, B, C, and D are listed in Table 1 for the various transport routes.

It can be seen in Fig. 3c that a change of the route results automatically in a different phase displacement coefficient in the entrance segment of the transport duct.

As the transport route becomes more complex, the displacement coefficient increases and this results in a reduced discharge efficacy at equal mass rates of air flow. For each route there is a minimum displacement coefficient, corresponding to the referred air velocity at which the transport takes place with the maximum weight concentration of the dust admixture.

An analysis of the obtained results shows that for each route there exists an optimum transport mode, at which the value of the displacement coefficient is minimum (see Fig. 3c) while the weight concentration of the dust admixture is maximum (see Fig. 3a).

Increasing the air velocity above the optimum will result in an increase of both the air-dust mixture porosity (see Fig. 3b) and the phase displacement (see Fig. 3c), which explains the already mentioned [2, 6] lower discharge efficacy and the lower weight concentration of the dust admixture.

Further experimental studies were made on large-scale models of a compressor pump with ducts 150 mm ($H = 28$ m) and 300 mm ($H = 13.5$ m, $L = 22$ m) in diameter.

The laboratory data obtained for these large-scale models have yielded a relation which with sufficient accuracy describes the heat losses in a pneumatic transport with a dense medium along a route including both vertical (H) and horizontal (L) segments:

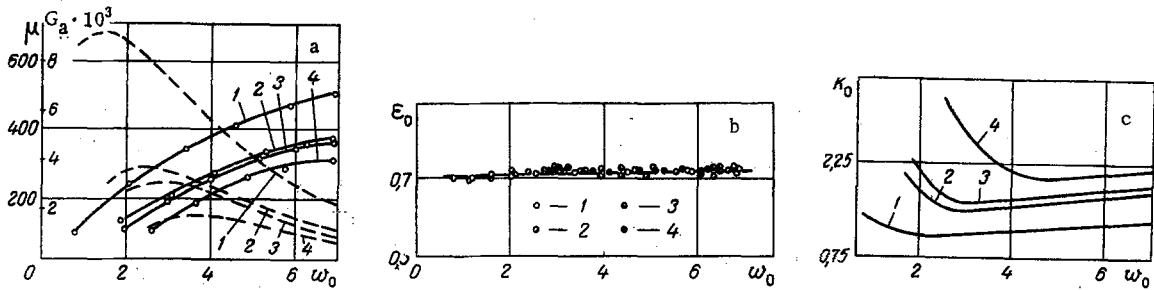


Fig. 3. a: Discharge efficacy (solid lines) G_m kg/h and concentration of dust admixture by weight u kg/kg; b: porosity of air-dust mixture ϵ_0 at transport duct entrance, c: phase displacement coefficient K_0 , all as functions of the referred air velocity w_0 m/sec. 1-4) Routes.

$$\Delta P = \lambda \frac{w_0^2}{2g} \gamma_a (1 - \epsilon_0) \frac{L_{\text{equ}}}{D_r^{0.3} d_p^{0.7}}, \quad (4)$$

where λ is a modified coefficient of resistance

$$\lambda = \frac{A^*}{\text{Fr}^m} + B^*,$$

A^* and B^* are constants, $A = 6730$, $B = 0.751 \cdot 10^{-3}$, m is a power exponent ($m = 3.54$), L_{equ} is the equivalent length of transport ($L_{\text{equ}} = \alpha_1 H + \alpha_2 L$ with $\alpha_1 = 2$ and $\alpha_2 = 0.3$).

NOTATION

D_T	is the duct diameter, m;
H	is the duct height, m;
L	is the duct length, m;
L_{equ}	is the equivalent duct length, m;
d_p	is the particle diameter, μm ;
G_a	is the air flow rate, kg/h;
G_m	is the discharge efficacy, kg/h;
ρ	is the air-dust mixture density, kg/m^3 ;
P_0, P_1, P_2, P_3	are the air pressure, N/m^2 ;
ΔP	is the pressure head loss, N/m^2 ;
w_a	is the air velocity, m/sec;
w_0	is the referred air velocity, m/sec;
w_m	is the particles' velocity, m/sec;
γ_m	is the specific weight of particles, kg/m^3 ;
γ_0	is the specific weight of air, kg/m^3 ;
λ	is the modified coefficient of resistance;
ϵ_0	is the porosity of air-dust mixture;
K_0	is the phase displacement coefficient;
$\text{Fr} = w_0/gd_p$	is the Froude number;
μ	is the weight concentration of dust admixture.

LITERATURE CITED

1. S. S. Zabrodskii, Hydrodynamics of and Heat Transfer in a Pseudoliquidified Medium [In Russian], Gosénergoizdat, Moscow-Leningrad (1963).
2. G. Belshof, Pneumatic Transport with a High Concentration of the Moved Material [Russian translation], Izd. Kolos, Moscow (1964).
3. M. B. Rivkin, Inzh. Fiz. Zh., 11, No. 1 (1966).
4. A. M. Gasparyan and R. E. Akopyan, Khim. Promyshl., No. 7 (1965).
5. I. Urban, Pneumatic Transport [Russian translation], Izd. Mashinostroenie, Moscow (1965).
6. V. B. Reznikov and M. B. Rivkin, Trudy Leningrad. Inst. Vodn. Transp., No. 89 (1967).
7. P. P. Artem'ev, M. B. Rivkin, and V. A. Sorochinskii, Trudy Leningrad. Inst. Vodn. Transp., No. 123 (1969).